9-5-2024

Angular Momentum Flow Without Anything Carrying It

Yakir Aharonov

Daniel Collins

Sandu Popescu

Angular Momentum Flow Without Anything Carrying It

Comments

Creative Commons License

Letter

Angular momentum flow without anything carrying it

Yakir Aharonov,[1,2,3] Daniel Collins [ ],[4] and Sandu Popescu [ ][4]

[1]*Schmid College of Science and Technology, Chapman University, Orange, California 92866, USA*
[2]*Institute for Quantum Studies, Chapman University, Orange, California 92866, USA*
[3]*School of Physics and Astronomy, Tel Aviv University, Tel Aviv 6997801, Israel*
[4]*H. H. Wills Physics Laboratory, University of Bristol, Tyndall Avenue, Bristol BS8 1TL, United Kingdom*

Transfer of conserved quantities between two remote regions is generally assumed to be a rather trivial process: a flux of particles carrying the conserved quantities propagates from one region to another. However, we demonstrate a flow of angular momentum from one region to another across a region of space in which there is a vanishingly small probability of any particles (or fields) being present. This shows that the usual view of how conservation laws work needs to be revisited.

Introduction. Conservation laws are some of the most important laws of physics. Stemming from basic symmetries of nature, they have been part of all physics theories, classical and quantum, relativistic and nonrelativistic. At the same time, the conceptual basis of the conservation laws seemed well established long ago. Yet quantum mechanics always comes with surprises. In the present paper, we analyze the way in which conserved quantities are exchanged between systems at two remote locations. Hitherto there appeared to be nothing interesting about this. For example, a flux of particles would carry angular momentum from one location to another. Here, however, we show that exchanges of conserved quantities could occur even across a region of space in which there is a vanishingly small probability of any particles (or fields) being present.

The results in this paper follow from the discovery of the Dynamic Cheshire Cat effect [1]. When describing a particle, we associate with it various properties: momentum, angular momentum, spin, energy, and so on. But in a gedanken experiment [2], which seems to come directly from the pages of *Alice in Wonderland*, it was shown that (in a pre- and post-selected setup) physical properties can be disembodied from the particles to which they belong. This "Quantum Cheshire Cat" phenomenon was experimentally confirmed in [3–6], and extended to more properties and particles in [7–13].

The original Cheshire Cat effect was considered in mostly "static" situations. More recently, however, it has been extended by showing that the disembodied property has a life of its own, evolving dynamically over time, making it a Dynamic Cheshire Cat [1].

The original motivation that led to the discovery of this dynamic effect was the desire for a better understanding of the issue of "counterfactual" information processing—counterfactual measurements [14–16], counterfactual computation [17–21], counterfactual cryptography [22,23], and in particular, counterfactual communication [24–39]. In all of these, information processing occurs without the particles that carry the information ever being present in the information processing devices. For example, in counterfactual communication a message is transmitted from Bob to Alice despite a vanishingly small probability of the particle ever being on Bob's side. That it is possible to transmit information without any physical system carrying it seems absurd, yet the counterfactual protocols seem to do precisely this. The main idea put forward in [1] is that there actually *is* an information carrier in the counterfactual effects, even though the *particle* that is supposed to be there is not present: the physical property that actually carries the information could be present in a "disembodied" way, i.e., without the particle to which it belongs, in a Cheshire-Cat-like effect.

The implications of this Dynamic Cheshire Cat effect, however, go well beyond its original motivation. The issue that interests us here is the connection with conservation laws.

As is well known, due to relativistic constraints, physical quantities are not only conserved but are conserved *locally*. That is, the conserved quantity moves from one place to a nearby place—technically, there is a current of the conserved quantity. One may imagine, however, a different mechanism, namely that a quantity is conserved by disappearing from one place while reappearing in a remote location. In classical mechanics, such a *global* conservation mechanism would be conceivable. But in relativistic mechanics, even if in one particular frame conservation could be obeyed in such a global manner, in a different frame conservation would be violated, since the disappearance in one place would not be simultaneous with reappearance in another place.

The relativistic requirement of local conservation is reflected also in the nonrelativistic quantum-mechanical limit in the well-known case of the local probability conservation. Not only is the total probability of finding the particle at some
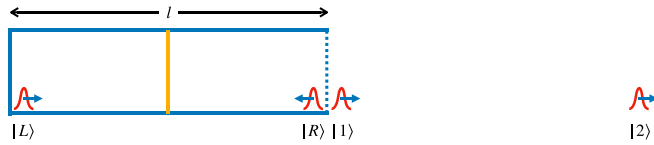
FIG. 1. The Dynamic Cheshire Cat. A spin-1/2 particle starts as a wave packet on the left side moving towards the right. In the middle of the box is a slightly transparent and highly reflective partition. The particle passes through the right side of the box when the spin, not shown here, is $|\uparrow_z\rangle$, and is reflected back towards the left when the spin is $|\downarrow_z\rangle$.

location always 1, i.e., $\int_{-\infty}^{\infty}|\Psi(x,t)|^2 dx = 1$, but Schrödinger's equation implies that the wave function changes in such a way that the probability distribution flows from one location to neighboring ones via the *probability current* $j = i(\Psi^* \frac{\partial \Psi}{\partial x} - \Psi \frac{\partial \Psi^*}{\partial x})$.

Although it is rarely discussed in textbooks (in fact, we found no mention of this at all), we naturally expect that all quantum-conserved quantities are conserved in this way.

The Dynamic Cheshire Cat effect described in [1], however, contains a dramatic twist since the information carrier quantity is a conserved quantity—angular momentum—and this flows from one location to neighboring ones without any probability current for the particle itself. How conservation acts in such a case is a fundamental issue.

Importantly, however, in [1] the disembodied conserved quantity transfer has only been proved *indirectly* with use of weak measurements. Here we give the first *direct* demonstration of the effect.

The paper is organized as follows. In the following section we describe the setup. In the third and fourth sections we prove our main result on angular momentum transfer from one side of a box to the wall on the other side, a transfer that takes place with infinitesimal probability of any particles transferring. In the fifth section we demonstrate that no linear momentum is transmitted to the wall during the process, further confirming that particles did not travel there. We end with our conclusions.

Dynamic Cheshire Cat. We first briefly review the Dynamic Cheshire Cat [1]. As shown in Fig. 1, this has a spin-1/2 particle moving in a box that has a slightly transparent (and highly reflective) partition in the middle. The left wall of the box is completely reflective, while the wall on the right is spin-dependent. It is fully transparent when the spin is $|\uparrow_z\rangle$, and completely reflective when the spin is $|\downarrow_z\rangle$. The particle starts at the left side of the box moving towards the right in the state $|L\rangle|\uparrow_z\rangle$. The particle will move back and forth in the box, as described below. We shall take the mass and velocity of the particle to be large enough that the spread of the wave packet remains small for the duration of the experiment.

At the end of the experiment we measure if the particle is in the left side of the box, where it was initially. When we find it there—which in our experiment will happen almost always—we measure its spin. It is the evolution of the spin that interests us.

More specifically, we define T to be the time for the particle to travel from the starting point to the central partition, reflect off it, continue to the left wall, reflect off that, and

return to its starting position. If the particle passes through the central partition, then since the right wall of the box is transparent to $|\uparrow_z\rangle$, at time T it will be just outside the right side of the box heading to the right, in a state we call $|1\rangle$. Once outside, the particle continues to move away from the box. This means that once the particle with spin $|\uparrow_z\rangle$ passes through the midpartition into the right side of the box, it never returns to the left side.

At time T the state has evolved as

$$|L\rangle|\uparrow_z\rangle \xrightarrow{T} (\cos\epsilon|L\rangle + i\sin\epsilon|1\rangle)|\uparrow_z\rangle, \qquad (1)$$

where $\epsilon = \pi/(2N)$ for some integer N is a small parameter describing the transmissivity of the central partition, and the phase factor i is picked up when passing through the central partition.

After $2N$ rounds at time $2NT$, the state will have evolved as

$$|L\rangle|\uparrow_z\rangle \xrightarrow{2NT} \left(\cos^{2N}\epsilon|L\rangle + i\sum_{k=1}^{2N}\sin\epsilon\cos^{2N-k}\epsilon|k\rangle\right)|\uparrow_z\rangle, \qquad (2)$$

where $|k\rangle$ is a state moving to the right outside the right wall at a distance kD from the left wall, where D is the length of the box. Since $\cos^{2N}(2\pi/N) = 1 - O(1/N)$, we have

$$|L\rangle|\uparrow_z\rangle \xrightarrow{2NT} |L\rangle|\uparrow_z\rangle + O(\epsilon). \qquad (3)$$

We can make these corrections as small as desired by setting N large. Thus we can make the probability of finding the particle in the left side of the box at the end of the experiment as close to 1 as desired.

Suppose instead we start with $|\downarrow_z\rangle$. The right wall now appears reflective, and we define the state of the particle at the right side of the box moving towards the left as $|R\rangle$. This evolves as

$$|L\rangle|\downarrow_z\rangle \xrightarrow{T} (\cos\epsilon|L\rangle + i\sin\epsilon|R\rangle)|\downarrow_z\rangle,$$

$$|R\rangle|\downarrow_z\rangle \xrightarrow{T} (\cos\epsilon|R\rangle + i\sin\epsilon|L\rangle)|\downarrow_z\rangle. \qquad (4)$$

At time $2NT$ this gives

$$|L\rangle|\downarrow_z\rangle \xrightarrow{2NT} [\cos(2N\epsilon)|L\rangle + i\sin(2N\epsilon)|R\rangle]|\downarrow_z\rangle = -|L\rangle|\downarrow_z\rangle. \qquad (5)$$

The particle has moved from the left side of the box to the right side and back again, with a phase factor of -1.

If we started instead with $|\uparrow_x\rangle = \frac{1}{\sqrt{2}}(|\uparrow_z\rangle + |\downarrow_z\rangle)$, we would see it flip to $|\downarrow_x\rangle$. And similarly $|\downarrow_x\rangle$ flips to $|\uparrow_x\rangle$. In itself this seems fine. Indeed, the spin can change because the particle tunnels to the right side of the box and encounters the right wall, where it undergoes a spin-dependent interaction.

But now comes the paradox. Suppose we start with $|\uparrow_z\rangle$ and make the wall almost reflective (i.e., take ϵ infinitesimally small) so that apart from an infinitesimal probability the particle does not leave the left side of the box during the experiment. Then we wait until time $2NT$, at which we find the particle on the left side of the box and measure the spin in the x direction, σ_x, and find it $|\uparrow_x\rangle$. What was σ_x at the start?

Spin $|\uparrow_z\rangle$ is a constant of motion so it does not change at all. The standard view is to say that it makes no sense to ask
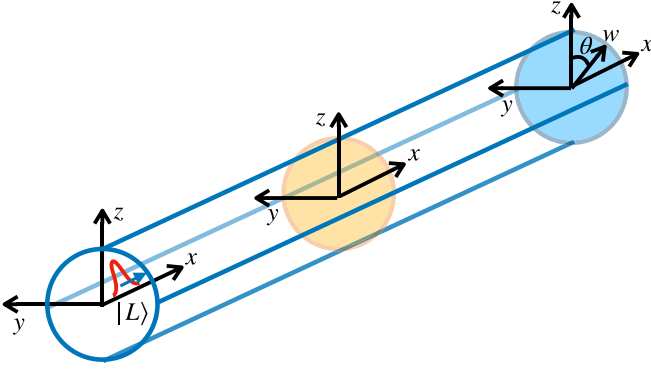
FIG. 2. Our thought experiment has a particle starting on the left, a highly reflective wall in the middle, and a spin-dependent wall that has a proper axis w, and which can rotate in the y-z plane, on the right.

the question about the value of σ_x; it is completely undefined when the spin is $|\uparrow_z\rangle$. However, in [1] it was argued that we should take the σ_x flip seriously, hence if at the end of the experiment we measure σ_x and find it $|\uparrow_x\rangle$, at the beginning it should have been $|\downarrow_x\rangle$. This implies the spin has flipped due to the wall on the right, despite the particle never being there. Similarly, if at the end of the experiment the σ_x measurement finds $|\downarrow_x\rangle$, at the beginning it should have been $|\uparrow_x\rangle$. This surprising conclusion was supported by showing that if one performs a weak measurement of σ_x at the start, a measurement that only disturbs the original experiment infinitesimally, then conditional on finding $|\uparrow_x\rangle$ at time $2NT$, we would find the spin as $|\downarrow_x\rangle$ at the start. While the measurement is weak and hence has a large uncertainly in any single experiment, it can be repeated many times to gather meaningful statistics.

In the next section, we go beyond weak measurement arguments and look directly at the change in angular momentum of the spin-dependent wall.

Angular Momentum Transfer. To study the angular momentum conservation including the change in angular momentum of the spin-dependent wall, we introduce our model, a modification of the setup of the Dynamic Cheshire Cat. As shown in Fig. 2, the spin-dependent wall has a "proper" axis, whose orientation is described by the unit vector **w** which lies in the plane of the wall. It is fully transparent for the particle if this has the spin parallel to **w** and oriented "up," and it is completely reflective if the spin is parallel to **w** and oriented "down."

Let the box be aligned with the x-axis, and the y- and z-axes perpendicular on it. The walls and the partition are orthogonal to the x-axis. The difference between our present arrangement and that in [1] is that we allow the spin-dependent wall to rotate. This can be realized by letting the wall have a circular form and be held by a circular frame in which it can slide. In practice, the "wall" can be constructed by a combination of a magnetic field and an electric potential, generated by an arrangement of a magnet and a capacitor, both of which could rotate together. We denote by θ the angle by which the wall is rotated around the x-axis, i.e., the angle between the wall's proper axis **w** and the z-axis. Finally, we take its moment of inertia to be very large, so that for the duration of

the experiment we can ignore its movement. This allows us to take the free Hamiltonian of the wall to be zero.

The reason we consider a rotating wall is that we want to be able to measure changes in the x-component of its angular momentum. In the original setup of [1], the wall's proper axis was taken to be along the z-axis. This makes the angular momentum $\hat{L}_x$ completely undefined, however, so a shift of it is unobservable. (This is also a non-normalizable state, and impossible to make in practice as there will always be a small deviation from perfect z in any real physical system.) For this reason, we take the state of the wall to be

$$|\Phi\rangle_w = \int_{-\pi}^{\pi} \Phi(\theta)|\theta\rangle_w d\theta, \tag{6}$$

where $\Phi(\theta)$ is a wave packet with nonzero spread.

The results below apply in fact for any $\Phi(\theta)$. We are interested, however, in the case in which $\Phi(\theta)$ is nonzero only in the region $-\Delta\theta \leqslant \theta \leqslant \Delta\theta$, which we can take as narrow as we want, to approximate our original experiment. (If θ is large, then there will be significant movement of the particle from the left side of the box into the right side, which spoils the original effect.) Note that $\Delta\theta$ is independent of ϵ: we can take both to be small independently of one another to achieve our desired behavior.

We will be interested in the case when initially the particle is in the left side of the box, with spin "up" along the z-axis. Putting this all together, the initial state is

$$|L\rangle|\uparrow_z\rangle|\Phi\rangle_w = \int_{-\pi}^{\pi} |L\rangle|\uparrow_z\rangle\Phi(\theta)|\theta\rangle_w d\theta. \tag{7}$$

The time evolution of the particle when the wall is in direction $|\theta\rangle$ is identical to that when the wall was in direction z (i.e., $\theta = 0$), Eqs. (3) and (5), but with the spin states also rotated to the corresponding directions $\uparrow_\theta$ and $\downarrow_\theta$ (see Appendix).

Suppose that, as in the original scenario, at time $2NT$ we measure whether the particle is in the left side of the box, and if we find it there (which happens almost certainly), we measure its x-spin component.

If we find the particle with spin $\sigma_x = +1$ the final state of the wall is (up to normalization) $|\Phi+\rangle_w$,

$$|\Phi+\rangle_w = \frac{1}{\sqrt{2}} \int_{-\pi}^{\pi} e^{-i\theta} \Phi(\theta)|\theta\rangle_w d\theta \tag{8}$$

(see Appendix).

We now arrive at the main result of the paper: The average of the x component of the angular momentum of the wall in the state $|\Phi+\rangle_w$ is $\langle\hat{L}_x\rangle_+ = \langle\hat{L}_x\rangle_0 - \hbar$, where $\langle\hat{L}_x\rangle_0$ is the initial average angular momentum [Eq. (A7)]. Therefore, the angular momentum of the wall has changed by $-\hbar$.

This is consistent with the prediction made in [1] where σ_x of the particle changes from $|\downarrow_x\rangle$ to $|\uparrow_x\rangle$, i.e., from $-\frac{1}{2}\hbar$ to $\frac{1}{2}\hbar$.

Similarly, when at the end of the experiment the particle is found on the left-hand side and the spin $\sigma_x = -1$, the final measurement of $\langle\hat{L}_x\rangle_- = \langle\hat{L}_x\rangle_0 + \hbar$, consistent with the prediction that σ_x of the particle changes from $|\uparrow_x\rangle$ to $|\downarrow_x\rangle$, i.e., from $\frac{1}{2}\hbar$ to $-\frac{1}{2}\hbar$.

Comment: the angular momentum transfer to the wall is independent of the initial state of the wall. This allows us to

approximate as closely as we want the original setup of [1], and assure that the perturbation that bounces off the wall can be made as small as we want, while the transfer of angular momentum to the wall remains finite in each individual case, $-\hbar$ or $+\hbar$.

Angular Momentum Flux. So far we showed that angular momentum in the x-direction of $\pm\hbar$ transfers from the particle to the spin-dependent wall in time $2NT$. Now we calculate the flux of this angular momentum, i.e., how much angular momentum the spin-dependent wall gains in each period of time T. If we did this by measuring the angular momentum of the wall at each time nT, for integer n where $1 \leqslant n \leqslant 2N$, we would disturb the experiment. Instead we consider having $2N$ walls, each placed at the right end of the box only for the period from $(n-1)T$ to nT. The flux is the momentum change on each individual wall. In Eq. (4) of the supplemental material (SM) [40], we show that when the particle is found on the left-hand side and the spin $\sigma_x = +1$, the flux is

$$\Delta\langle\hat{L}_x\rangle_n \approx -\hbar\sin\frac{(2n-1)\pi}{4N}\sin\frac{\pi}{4N}. \qquad (9)$$

It varies over half a period of a sine wave, $\sin\frac{n\pi}{2N}$, for $1 \leqslant n \leqslant 2N$. The sum over all n matches the result from the previous section, $-\hbar$ [SM Eq. (5) [40]]. The flux also matches that calculated in Eq. (39) of [1] (in that paper, a factor $\hbar/2$ for the particle being spin-1/2 was omitted). That calculation was based on weak values measured in the right side of this box: this one is direct as it is based on the angular momentum received by the spin-dependent wall over time.

Linear Momentum Transfer. In [1] and the present article, it was argued that there is no particle traveling towards the wall, *only* a "disembodied" spin. There is, however, a fundamental consequence of this that was not noticed in [1]: there should be no linear momentum transfer to the wall.

When the wall is precisely oriented along z, it is totally transparent to the particle (which is prepared $|\uparrow_z\rangle$), so it exerts no force on it. However, this orientation implies there are no observational angular momentum transfer effects, so we gave the wall an initial spread in the angular direction. Now, however, the particle may sometimes collide with the wall. We have to show that the observed angular momentum transfer is not due to these collisions. We will prove this by making the linear momentum transfer arbitrarily small while keeping the exchange of angular momentum unchanged at $\pm\hbar$.

Thus far the wall was considered to be at a precise location along the x-axis. To make a change in its linear momentum observable, we now take the position of the wall to be a wave packet narrowly localized around the right end of the box. We denote this as $\Psi(x_w)$, centered around $x_w = 0$, and only nonzero for $-\Delta x_w \leqslant x_w \leqslant \Delta x_w$. The initial state of the wall is then

$$|\Phi\rangle|\Psi\rangle = \int_{-\pi}^{\pi}\Phi(\theta)|\theta\rangle_w d\theta\int_{-\Delta x_w}^{\Delta x_w}\Psi(x_w)|x_w\rangle dx_w. \qquad (10)$$

In Sec. I of the SM [40], we calculate the average linear momentum transfer after state evolution. This is [SM Eq. (9) [40]]

$$\langle\hat{p}_f\rangle - \langle\hat{p}_i\rangle = 2p_0\int\left|\sin\left(\frac{\theta}{2}\right)\Phi(\theta)\right|^2 d\theta + O(\Delta x_w), \quad (11)$$

where p_0 is the initial momentum of the particle, and Δx_w is the uncertainty of the position of the wall. The change in the linear momentum of the wall goes to zero when $\Delta\theta$ and Δx_w are small, more precisely $\Delta x_w \ll \hbar/(2Np_0)$, which we achieve by choosing Δx_w after N is chosen. This ensures that even after all $2N$ rounds, the wave packets remain to a good approximation in the same phase relation as in the original unperturbed experiment (SM Sec. II [40]). Crucially, the angular momentum transfer remains $\pm\hbar$ (SM Sec. II [40]). Thus in every experiment there is a fixed angular momentum transfer and negligible linear momentum transfer.

Conclusion. In the present paper, we have given direct evidence of angular momentum transfer between two remote locations across a region of space where there is a vanishingly small probability of any particles (or fields) being present. Although presented in the particular case of angular momentum, it seems obvious that the same phenomenon allows for disembodied transfer of arbitrary conserved quantities. Our results provide a new understanding of the way conservation laws work.

Appendix: Angular momentum transfer calculation. Here we calculate the change in angular momentum of the spin-dependent wall in the x-direction, as discussed in the section on angular momentum transfer. The initial state is, as given in Eq. (7),

$$|L\rangle|\uparrow_z\rangle|\Phi\rangle_w = \int_{-\pi}^{\pi}|L\rangle|\uparrow_z\rangle\Phi(\theta)|\theta\rangle_w d\theta. \qquad (A1)$$

The evolution of the particle was given in Eqs. (3) and (5) for the case in which the wall was oriented "up" z. Since the z direction was nothing special, when the wall is oriented along θ we can write similar expressions for when the spin was initially polarized $|\uparrow_\theta\rangle$ and $|\downarrow_\theta\rangle$:

$$|L\rangle|\uparrow_\theta\rangle \xrightarrow{2NT} |L\rangle|\uparrow_\theta\rangle + O(\epsilon),$$
$$|L\rangle|\downarrow_\theta\rangle \xrightarrow{2NT} -|L\rangle|\downarrow_\theta\rangle. \qquad (A2)$$

Note that since the direction θ is in the y-z plane, the states $|\uparrow_z\rangle$ and $|\downarrow_z\rangle$ can be decomposed as

$$|\uparrow_z\rangle = \cos\frac{\theta}{2}|\uparrow_\theta\rangle + i\sin\frac{\theta}{2}|\downarrow_\theta\rangle,$$
$$|\downarrow_z\rangle = i\sin\frac{\theta}{2}|\uparrow_\theta\rangle + \cos\frac{\theta}{2}|\downarrow_\theta\rangle. \qquad (A3)$$

The time evolution then is

$$\int_{-\pi}^{\pi}|L\rangle|\uparrow_z\rangle\Phi(\theta)|\theta\rangle_w d\theta$$
$$= \int_{-\pi}^{\pi}|L\rangle\left(\cos\frac{\theta}{2}|\uparrow_\theta\rangle + i\sin\frac{\theta}{2}|\downarrow_\theta\rangle\right)\Phi(\theta)|\theta\rangle_w d\theta$$
$$\xrightarrow{2NT}\int_{-\pi}^{\pi}|L\rangle\left(\cos\frac{\theta}{2}|\uparrow_\theta\rangle - i\sin\frac{\theta}{2}|\downarrow_\theta\rangle\right)\Phi(\theta)|\theta\rangle_w d\theta$$
$$+ O(\epsilon), \qquad (A4)$$

where we used Eq. (A2).

Suppose we measure at the end of this evolution whether the particle is in the left side of the box or not, and if we find it there we measure the spin along the x-axis. The spin measurement can yield $\sigma_x = +1$ or -1. We are interested in the average angular momentum of the wall for each of these two outcomes.

When the particle is found in the left-hand side and the spin $\sigma_x = +1$, the state of the wall, $|\Phi+\rangle_w$, is (up to normalization)

$$\int_{-\pi}^{\pi} \left(\cos\frac{\theta}{2}\langle\uparrow_x|\uparrow_\theta\rangle - i\sin\frac{\theta}{2}\langle\uparrow_x|\downarrow_\theta\rangle \right)\Phi(\theta)|\theta\rangle_w d\theta$$

$$= \frac{1}{\sqrt{2}}\int_{-\pi}^{\pi} e^{-i\theta}\Phi(\theta)|\theta\rangle_w d\theta, \qquad (A5)$$

where we used the scalar products

$$\langle\uparrow_x|\uparrow_\theta\rangle = \langle\uparrow_x|\left(\cos\frac{\theta}{2}|\uparrow_z\rangle - i\sin\frac{\theta}{2}|\downarrow_z\rangle \right)$$

$$= \frac{1}{\sqrt{2}}\left(\cos\frac{\theta}{2} - i\sin\frac{\theta}{2} \right) = \frac{1}{\sqrt{2}}e^{-i\frac{\theta}{2}},$$

$$\langle\uparrow_x|\downarrow_\theta\rangle = \langle\uparrow_x|\left(\cos\frac{\theta}{2}|\downarrow_z\rangle - i\sin\frac{\theta}{2}|\uparrow_z\rangle \right)$$

$$= \frac{1}{\sqrt{2}}\left(\cos\frac{\theta}{2} - i\sin\frac{\theta}{2} \right) = \frac{1}{\sqrt{2}}e^{-i\frac{\theta}{2}}. \qquad (A6)$$

The average of the x component of the angular momentum of $|\Phi+\rangle_w$, $\langle\hat{L}_x\rangle_+$ is $\langle\hat{L}_x\rangle_0 - \hbar$, where $\langle\hat{L}_x\rangle_0$ is the initial average angular momentum. Indeed

$$\langle\hat{L}_x\rangle_+ = \int_{-\pi}^{\pi} e^{i\theta}\Phi^*(\theta)(-i\hbar)\frac{\partial}{\partial\theta}e^{-i\theta}\Phi(\theta)d\theta$$

$$= \int_{-\pi}^{\pi} \Phi^*(\theta)(-i\hbar)\frac{\partial}{\partial\theta}\Phi(\theta)d\theta - \hbar$$

$$\times \int_{-\pi}^{\pi} \Phi^*(\theta)\Phi(\theta)d\theta = \langle\hat{L}_x\rangle_0 - \hbar. \qquad (A7)$$

Now to calculate the change in angular momentum, we need to take the difference between the initial and final momentum. It is tempting to simply state that the initial angular momentum of the wall along the x-axis is $\langle\hat{L}_x\rangle_0$. However, we have made a postselection of $\langle\uparrow_x|$ that changed the initial angular momentum of the particle along the x-axis from 0 to $-\frac{1}{2}\hbar$. Therefore, we need to check whether the initial angular momentum of the wall, conditional on the postselection, has also changed.

To do this, we start from the final state of the particle, $\langle\uparrow_x|$, and the final state of the wall as given in Eq. (A5), and we evolve the joint state backwards in time to the start. Then we preselect on the particle starting $|\uparrow_z\rangle$, and we calculate the initial angular momentum of the wall. This goes as follows:

$$\frac{1}{\sqrt{2}}\int_{-\pi}^{\pi} e^{i\theta}\Phi^*(\theta)\langle\theta|_w d\theta\langle\uparrow_x|$$

$$= \frac{1}{2}\int_{-\pi}^{\pi} e^{i\theta}\Phi^*(\theta)\langle\theta|_w d\theta\left(\langle\uparrow_z| + \langle\downarrow_z|\right)$$

$$= \frac{1}{2}\int_{-\pi}^{\pi} e^{i\theta}\Phi^*(\theta)\langle\theta|_w d\theta e^{-i\frac{\theta}{2}}(\langle\uparrow_\theta| + \langle\downarrow_\theta|)$$

$$\xrightarrow{2nT} \frac{1}{2}\int_{-\pi}^{\pi} e^{i\frac{\theta}{2}}\Phi^*(\theta)\langle\theta|_w d\theta(\langle\uparrow_\theta| - \langle\downarrow_\theta|)$$

$$= \frac{1}{2}\int_{-\pi}^{\pi} e^{i\frac{\theta}{2}}\Phi^*(\theta)\langle\theta|_w d\theta e^{-i\frac{\theta}{2}}\left(\langle\uparrow_z| - \langle\downarrow_z|\right)$$

$$\to \frac{1}{2}\int_{-\pi}^{\pi} \Phi^*(\theta)\langle\theta|_w d\theta \text{ under preselection on } |\uparrow_z\rangle, \quad (A8)$$

i.e., the postselection has not changed the original state of the wall.

Thus the initial angular momentum of the wall conditional on the postselection is still $\langle\hat{L}_x\rangle_0$, and the change in the angular momentum along the x-axis of the wall is $-\hbar$.

[1] Y. Aharonov, E. Cohen, and S. Popescu, A dynamical quantum Cheshire Cat effect and implications for counterfactual communication, Nat. Commun. **12**, 4770 (2021).

[2] Y. Aharonov, S. Popescu, D. Rohrlich, and P. Skrzypczyk, Quantum Cheshire Cats, New J. Phys. **15**, 113015 (2013).

[3] T. Denkmayr, H. Geppert, S. Sponar, H. Lemmel, A. Matzkin, J. Tollaksen, and Y. Hasegawa, Observation of a quantum Cheshire Cat in a matter-wave interferometer experiment, Nat. Commun. **5**, 4492 (2014).

[4] J. M. Ashby, P. D. Schwarz, and M. Schlosshauer, Observation of the quantum paradox of separation of a single photon from one of its properties, Phys. Rev. A **94**, 012102 (2016).

[5] Y. Kim, D.-G. Im, Y.-S. Kim, S.-W. Han, S. Moon, Y.-H. Kim, and Y.-W. Cho, Observing the quantum Cheshire Cat effect with noninvasive weak measurement, npj Quantum Inf. **7**, 13 (2021).

[6] J.-K. Li, K. Sun, Y. Wang, Z.-Y. Hao, Z.-H. Liu, J. Zhou, X.-Y. Fan, J.-L. Chen, J.-S. Xu, C.-F. Li, and G.-C. Guo, Experimental demonstration of separating the wave-particle duality of a single photon with the quantum Cheshire Cat, Light: Sci. Appl. **12**, 18 (2023).

[7] Y. Guryanova, N. Brunner, and S. Popescu, The complete quantum Cheshire Cat, arXiv:1203.4215.

[8] I. Ibnouhsein and A. Grinbaum, Twin quantum Cheshire photons, arXiv:1202.4894.

[9] A. D. Lorenzo, Hunting for the quantum Cheshire Cat, arXiv:1205.3755.

[10] A. K. Pan, Disembodiment of arbitrary number of properties in quantum Cheshire Cat experiment, Eur. Phys. J. D **74**, 151 (2020).

[11] D. Das and A. K. Pati, Teleporting grin of a quantum Chesire Cat without cat, arXiv:1903.04152.

[12] D. Das and A. K. Pati, Can two quantum Cheshire Cats exchange grins? New J. Phys. **22**, 063032 (2020).

[13] Z.-H. Liu, W.-W. Pan, X.-Y. Xu, M. Yang, J. Zhou, Z.-Y. Luo, K. Sun, J.-L. Chen, J.-S. Xu, C.-F. Li, and G.-C. Guo, Experimental exchange of grins between quantum Cheshire Cats, Nat. Commun. **11**, 3006 (2020).

[14] A. Elitzur and L. Vaidman, Quantum-mechanical interaction-free measurements, Found. Phys. **23**, 987 (1993).

[15] P. Kwiat, H. Weinfurter, T. Herzog, A. Zeilinger, and M. A. Kasevich, Interaction-free measurement, Phys. Rev. Lett. **74**, 4763 (1995).

[16] L. Hardy, Quantum mechanics, local realistic theories, and lorentz-invariant realistic theories, Phys. Rev. Lett. **68**, 2981 (1992).

[17] R. Jozsa, Quantum effects in algorithms, in *Quantum Computing and Quantum Communications*, edited by C. Williams, Lecture Notes In Computer Science Vol. 1509, (Springer, Berlin, Heidelberg, 1999), pp. 103–112.

[18] G. Mitchison and R. Jozsa, Counterfactual computation, Proc. R. Soc. London Ser. A **457**, 1175 (2001).

[19] O. Hosten, M. Rakher, J. Barreiro, N. Peters, and P. Kwiat, Counterfactual quantum computation through quantum interrogation, Nature (London) **439**, 949 (2006).

[20] L. Vaidman, Impossibility of the counterfactual computation for all possible outcomes, Phys. Rev. Lett. **98**, 160403 (2007).

[21] G. Mitchison and R. Jozsa, The limits of counterfactual computation, arXiv:quant-ph/0606092.

[22] T.-G. Noh, Counterfactual quantum cryptography, Phys. Rev. Lett. **103**, 230501 (2009).

[23] G.-C. Guo and B.-S. Shi, Quantum cryptography based on interaction-free measurement, Phys. Lett. A **256**, 109 (1999).

[24] H. Salih, Z.-H. Li, M. Al-Amri, and M. S. Zubairy, Protocol for direct counterfactual quantum communication, Phys. Rev. Lett. **110**, 170502 (2013).

[25] H. Salih, Protocol for counterfactually transporting an unknown qubit, Front. Phys. **3**, 94 (2016).

[26] R. B. Griffiths, Particle path through a nested Mach-Zehnder interferometer, Phys. Rev. A **94**, 032115 (2016).

[27] L. Vaidman, Comment on "Particle path through a nested Mach-Zehnder interferometer," Phys. Rev. A **95**, 066101 (2017).

[28] H. Salih, Comment on "Particle path through a nested Mach-Zehnder interferometer," Phys. Rev. A **97**, 026101 (2018).

[29] R. B. Griffiths, Reply to "Comment on 'Particle path through a nested Mach-Zehnder interferometer'," Phys. Rev. A **95**, 066102 (2017).

[30] R. B. Griffiths, Reply to "Comment on 'Particle path through a nested Mach-Zehnder interferometer,'" Phys. Rev. A **97**, 026102 (2018).

[31] L. Vaidman, Counterfactuality of 'counterfactual' communication, J. Phys. A **48**, 465303 (2015).

[32] D. R. M. Arvidsson-Shukur, A. N. O. Gottfries, and C. H. W. Barnes, Evaluation of counterfactuality in counterfactual communication protocols, Phys. Rev. A **96**, 062316 (2017).

[33] L. Vaidman, Comment on "Protocol for direct counterfactual quantum communication," Phys. Rev. Lett. **112**, 208901 (2014).

[34] H. Salih, Z. H. Li, M. Al-Amri, and M. S. Zubairy, Reply to "Comment on 'Protocol for direct counterfactual quantum communication'," Phys. Rev. Lett. **112**, 208902 (2014).

[35] A. Danan, D. Farfurnik, S. Bar-Ad, and L. Vaidman, Asking photons where they have been, Phys. Rev. Lett. **111**, 240402 (2013).

[36] L. Vaidman, Past of a quantum particle, Phys. Rev. A **87**, 052104 (2013).

[37] Y. Aharonov and L. Vaidman, Modification of counterfactual communication protocols that eliminates weak particle traces, Phys. Rev. A **99**, 010103(R) (2019).

[38] Y. Aharonov and D. Rohrlich, What is nonlocal in counterfactual quantum communication? Phys. Rev. Lett. **125**, 260401 (2020).

[39] L. Vaidman, Analysis of counterfactuality of counterfactual communication protocols, Phys. Rev. A **99**, 052127 (2019).

[40] See Supplemental Material at http://link.aps.org/supplemental/10.1103/PhysRevA.110.L030201 for 1. The calculation of the Angular Momentum Flux and 2. The calculation of the Linear Momentum Transfer.